Model Dependence of the Anisotropic Structuring of Solvent Water around Sugars in Molecular Dynamics Simulations

Qiang Liu and J. W. Brady*

Department of Food Science, Stocking Hall, Cornell University, Ithaca, New York 14853

Received: September 26, 1996; In Final Form: November 6, 1996[⊗]

Microcanonical ensemble molecular dynamics simulations have been used to examine the model dependence of the computed three-dimensional structuring which the typical sugar D-xylose imposes on surrounding solvent molecules in aqueous solution. The structuring imposed on water by biological solutes is quite complex, due to the complicated mix of chemical functionalities found in typical biopolymers, and has proven difficult to probe experimentally. Computer simulations have been the principal source of spatially resolved information about the solvent structuring about particular solutes, and previous simulations of this sugar have found configuration-dependent solvent structuring which appears to explain an important experimentally determined physical characteristic of the molecule, its anomeric ratio. Well-defined first and second solvation shells are observed around the sugar molecule with specific locations determined by the arrangement of functional groups in the solute. Here we examine the dependence of this calculated solvent structuring upon the solvent model employed by comparing simulations using the TIP3P and SPC/E water force fields. The solvent structuring is found to be qualitatively the same in both simulations and is primarily determined by geometric constraints determined by the solute topology.

I. Introduction

The geometric requirements of the hydrogen bonds made by water molecules in aqueous solutions impart considerable structure to those water molecules surrounding complex molecular solutes. This structuring varies as a function of the specific topology of the solute molecule and is responsible for many of the properties of aqueous solutions. Unfortunately, it is difficult or often impossible to determine the details of this structuring experimentally. Neutron or X-ray scattering from liquids has been successfully used to determine spherically symmetric pair distribution functions for water structuring around ions[1] and rare gases,[2] but it is much more difficult to extract non-spherically averaged information about the solvent structure around complex molecular solutes such as biopolymers. However, computer simulations can be used to model such structuring theoretically and have been extremely useful in probing aqueous systems.[3−10]

Recently we reported MD simulations of solvent structuring around various pentose sugar molecules.[11,12] Because of their complex geometry, with hydrophobic and hydrophilic functional groups in close proximity, the sugars make good models of biological hydration. All of the pentoses are structural isomers of one another, differing only in the stereochemistry at the various asymmetric carbon atoms,[13] yet they have distinct solvation properties.[14] In our previous studies, the three-dimensional structuring of the hydrogen-bonded first-shell solvent was found to vary with sugar configuration,[12] and in the case of the anomeric carbon, this differing hydration was found to play a role in determining the equilibrium concentrations of the two anomeric forms. Analysis of simulations of different sizes confirmed that the calculated structure was not an artifact of the application of periodic boundary conditions to a system of small size. However, the possibility remains that the calculated solvent structuring results from the specific solvent model used, although the indirect correlation with experiment would seem to suggest that the structuring is physically realistic.

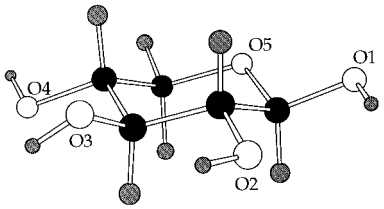

Figure 1. β-D-xylopyranose, with the numbering of the oxygen atoms indicated for clarity.

The previously reported sugar simulations employed the TIP3P water potential energy model.[15] Although widely used in MD simulations of aqueous solutions, this potential energy function is known to produce less tetrahedral structuring than other water models; in particular, the radial distribution function for pure water modeled with this function has only a weak second peak. Another widely used water model, the SPC energy function,[16] gives an oxygen radial distribution for pure water which is in closer agreement with the experimentally measured function. A recent revision of this model, the SPC/E energy function,[17] also gives good agreement with experimental values for the binding energy and density of pure water, as well as a translational self-diffusion coefficient in close agreement with the experimental value. We report here a comparison of the solvent structuring observed in MD simulations of the pyranoid pentose monosaccharide β-D-xylopyranose using the TIP3P and SPC/E water models.

II. Methods

For the present comparison, a new MD simulation was performed of β-D-xylopyranose (Figure 1) in a periodic cubic box 24.7711 Å in length containing 502 SPC/E water molecules, corresponding to more than three solvation shells in the primary box. All simulation protocols were the same as in our previous simulation of the same sugar in TIP3P water.[12] The calculations were made using the molecular mechanics program CHARMM,[18]

* To whom correspondence should be addressed.
[⊗] Abstract published in *Advance ACS Abstracts,* February 1, 1997.

S1089-5647(96)02979-3 CCC: $14.00

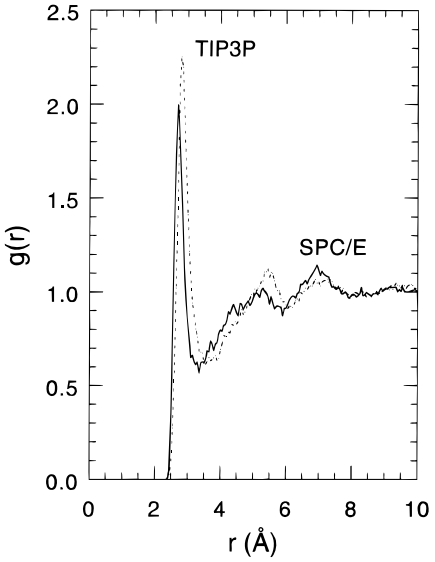

Figure 2. Pair distribution function for water oxygen atoms around the O3 hydroxyl oxygen atom as calculated from the simulation of β-D-xylopyranose in SPC/E water, compared with that calculated previously in TIP3P water (dashed line).

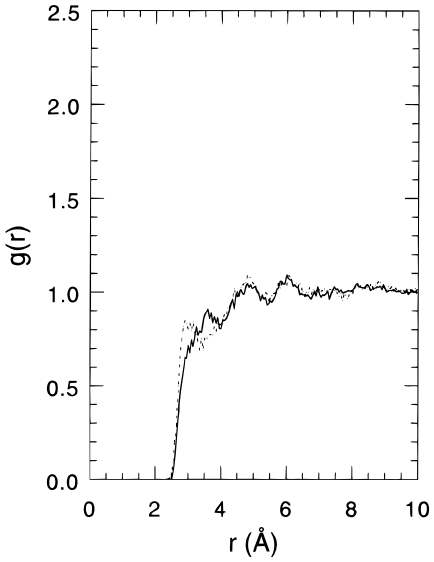

Figure 3. Pair distribution function for water oxygen atoms around the ring oxygen atom O5, as calculated from the SPC/E MD simulation.

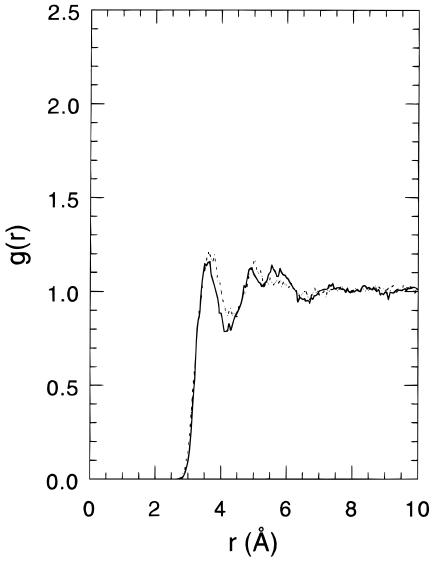

Figure 4. Pair distribution function for water oxygen atoms around the C3 atom, as calculated from the SPC/E MD simulation.

and the sugar potential energy was modeled using a CHARMM-type force field developed for carbohydrates.[19] After 30 ps of equilibration, the equations of motion for the system were computed in the microcanonical ensemble for 150 ps at a temperature of 300 K. Equations of motion were integrated using a Verlet integrator[20] with a step size of 1 fs. Chemical bonds involving hydrogen atoms were kept fixed using the constraint algorithm SHAKE,[21] which was also used to keep the water molecules rigid. Nonbond interactions were made to go smoothly to zero through the application of switching functions[18] computed on a group-by-group basis[22] between the distances of 10.0 and 11.0 Å.

The anisotropic structuring of solvent water molecules around the xylose was averaged as before[11,12] and compared with the TIP3P simulation. The relatively rigid rings of pyranoid sugars[9,23,24] keep the hydroxyl groups and aliphatic protons in these molecules at approximately fixed relative orientations. No transitions away from the crystallographic $^4C_1$ ring conformation occurred in the simulations, in agreement with NMR results.[25] The only thermally accessible conformational freedom consists of hydroxyl proton rotations (in xylose, with four hydroxyl groups, there are $3^4 = 81$ possible staggered conformational substates for these groups). Exploiting this relative rigidity of the sugar ring, each coordinate set of the MD simulation can be translated and rotated so as to achieve the best least-squares overlap of the instantaneous positions of the six ring atoms with their initial positions, to remove the effects of solute diffusion and rotation. This same coordinate transformation can be applied to all solvent molecules and their periodic images. A Gaussian function centered on each water oxygen atom was used to approximate the distribution of electrons for each molecule, and the spatially resolved average solvent electronic density relative to a frame fixed on the sugar ring was calculated and contoured with the program CHAIN[26] to allow the location of regions of space around the sugar which have higher and lower than bulk density as a result of structuring of the solvent by the functional groups of the solute.

III. Results and Discussion

In general, the solvent structuring in the present simulation is qualitatively similar to that observed previously but differs quantitatively in a manner consistent with the known differences in behavior of the two water models. Figures 2−4 display the pair distribution functions for water molecules around the O3 hydroxyl oxygen atom, the O5 ring oxygen atom, and the C3 carbon atom. These functions are qualitatively very similar to those calculated for TIP3P solvent. The first peak in the SPC/E function for the O3 hydroxyl oxygen (Figure 2) has a somewhat lower intensity, with a maximum at 2.7 Å of only 2.00, compared with a maximum of 2.25 for the TIP3P simulation. The distribution displays a deep minimum around 3.4 Å, as in the TIP3P function, a broad second peak around 5.3 Å, and a third peak around 7.0 Å. All of these features are markedly more pronounced than for the oxygen−oxygen pair distribution function in pure water, as is the case for the TIP3P simulation. However, as in the TIP3P case, much of the apparent structuring in this function is an artifact resulting from the radial averaging over the full 4π solid angle. The pronounced second peak is largely due to the distal first peaks of the adjacent hydroxyl groups, which coincidentally lie at the same distance as a second peak in this function would be expected due to the relatively rigid structure of the sugar ring. The unexpectedly deep first minimum, which is almost identical in the two simulations,

TABLE 1: Number of Hydrogen Bonds to Solvent Made by Each Oxygen Atom of the Xylose Solute, Either as a Donor or Acceptor, As Calculated from Both Simulations Using Conventional Geometric Criteria,[10] for Three Different Cutoff Values of the O−H···O Angle[a]

solute atom	120°		130°		140°	
	SPC/E	TIP3P	SPC/E	TIP3P	SPC/E	TIP3P
O1	2.67	2.85	2.42	2.23	2.18	1.61
O2	2.40	2.70	2.13	2.07	1.87	1.46
O3	2.58	2.63	2.32	2.08	2.07	1.52
O4	2.57	2.70	2.35	2.13	2.13	1.57
O5	0.87	0.82	0.67	0.58	0.51	0.37
total	11.09	11.70	9.89	9.09	8.76	6.53

[a] In all cases the distance cutoff used was 3.5 Å.

results then from averaging across the ring, where water molecules are excluded by clashes with the ring atoms. Similarly, as in the TIP3P case, the unexpectedly significant third peak is almost entirely due to the first peaks for the O1 and O5 atoms on the opposite side of the sugar ring. This limitation of radially averaged distribution functions is well understood[27] and was discussed in our previous report.[12]

The distribution function for SPC/E water oxygen atoms around the sugar O5, displayed in Figure 3, has almost no first peak and that for the TIP3P water is very weak, due to the reduced ability of the ring oxygen to compete for hydrogen bond partners as a result of its lower charge. Again, the two functions are qualitatively very similar. The C3 distribution displayed in Figure 4 features the broad first peak, centered around 3.6 Å, which is characteristic of hydrophobic solutes. This function is also similar to that seen in the TIP3P calculation, but the features are somewhat more regular than in that case, perhaps indicating a greater hydrophobic structuring imposed on the adjacent water with this model. Such a result would seem reasonable, since the water molecules in this shell are hydrogen bonded only to other water molecules, rather than to the solute, and the SPC/E model, which produces more structure in water−water interactions, might be expected to give more structuring in this case.

The two simulations are also similar in their numbers of hydrogen bonds made to solvent. Table 1 lists the average number of solvent hydrogen bonds made by each oxygen atom as calculated from the simulations using geometric criteria. A water molecule was considered to be hydrogen bonded to a particular hydroxyl group if its oxygen atom was less than 3.5 Å away from the hydroxyl oxygen atom, and if the O−H···O angle was greater than the specified angular cutoff. As can be seen, the numbers calculated from the two simulations are again qualitatively very similar, but the number of solvent hydrogen bonds in the SPC/E simulation was consistently smaller for each hydroxyl group using the 120° angle cutoff, while it was larger for the ring oxygen atom. Summed over all of the oxygen atoms in both simulations, the sugar makes 0.61 more hydrogen bonds to solvent molecules in the TIP3P simulation than in the SPC/E simulation, using the geometric criteria with a 120° angle cutoff. However, the total binding energy of the sugar to the water is much larger in the SPC/E simulation, −73.4 vs −66.2 kcal/mol in the TIP3P simulation, both computed using the same nonbonded cutoff distances and switching functions. One reason for this difference appears to be that the more structured SPC/E water results in more regular hydrogen bonds to the solvent, with more favorable energies, than in the TIP3P simulation, where the less structured waters can make geometrically more distorted hydrogen bonds, giving a larger absolute number, but with less favorable energies. This interpretation is confirmed by the numbers of hydrogen bonds for the two simulations listed in Table 1 for more strict angle cutoff definitions. Using the more linear cutoff criterion of 140°, the sugar makes 2.23 more hydrogen bonds to solvent in the SPC/E simulation than in the TIP3P simulation.

Figure 5 displays the three-dimensional structuring of water around the sugar molecules by contouring of the solvent density around the xylose molecule as calculated from the two simulations. The regions enclosed by the contour grid have solvent densities at least 50% greater that the bulk density. As can be seen, the distribution is highly anisotropic in both simulations, due to the overlapping hydration requirements of the adjacent

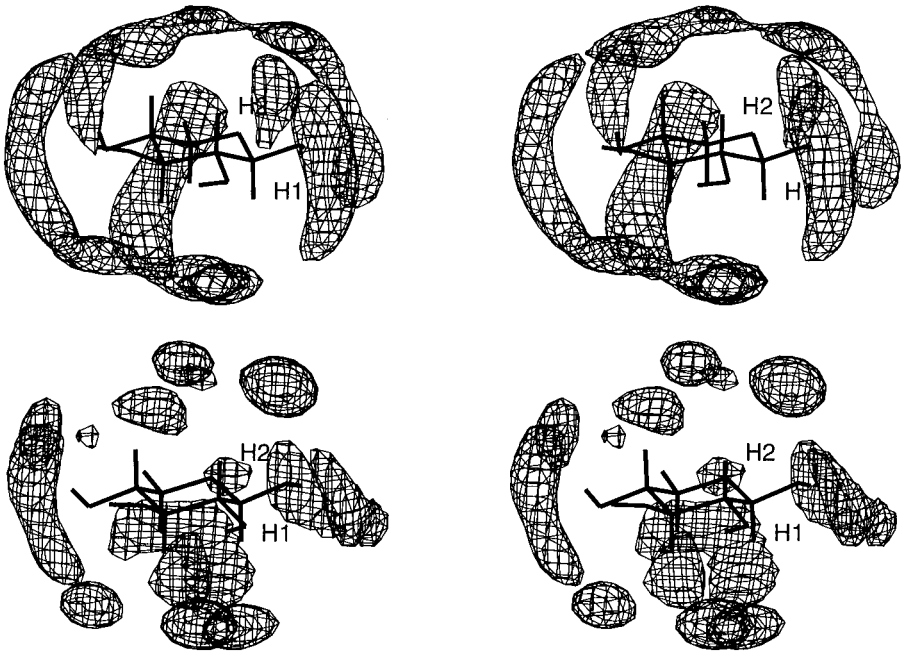

Figure 5. Stereo pairs showing contours of solvent electronic density around a β-D-xylopyranose molecule as calculated from MD simulations. The contour grid encloses those regions with a density 50% greater than the bulk density. The sugar structure is indicated, and two atoms are labeled in each structure for reference. (a, top) The density calculated from the previously reported TIP3P simulation; (b, bottom) the density calculated from the present SPC/E simulation.

groups of the solute. In the previously reported TIP3P simulation, at the selected contour level, the high-density regions consist of long tube-shaped clouds located between adjacent pairs of hydroxyl groups around the periphery of the ring. These banana- or tube-shaped clouds have some of the character of a bent dumbbell with greater density above and below the ring, and relatively less density in the plane of the ring. These regions are primarily occupied by water molecules making two simultaneous hydrogen-bond-like interactions with the solute, one with each of the adjacent hydroxyl groups. The clouds of density are located approximately at constant azimuthal angle and distance from the center of the ring, except at the extreme top and bottom of the clouds. Because of the geometry of the sugar, it is generally not possible for the water molecules to simultaneously make two ideal hydrogen bonds to the adjacent hydroxyl groups,[10] so that many of these interactions have O−H−O angles distorted away from linearity. At the top and bottom of these clouds the regions of density associated with waters hydrogen bonded to the solute merge with clouds of density associated with water molecules solvating the hydrophobic C−H groups. These water molecules, which generally make no hydrogen bonds to the solute, are oriented differently from the hydrogen-bonding solvent molecules and are located at somewhat greater distances from the center of the ring, as is known from studies of the behavior of nonpolar solutes in water.[2,3]

It can be seen by comparing the densities displayed for the two simulations that in many respects they are qualitatively the same. The SPC/E simulation exhibits somewhat more regular structuring, so that the tubes of density tend, at this contour level, to break up into smaller, more localized concentrations of density (the tube structure is recovered when contoured at a lower density). Each hydroxyl group has three such clouds at roughly tetrahedral positions corresponding to the directions of the hydroxyl proton in its three staggered rotameric conformations. The TIP3P simulation also has this qualitative feature, but the densities must be contoured at a higher level for it to be fully detected in that simulation. Thus the simulations are qualitatively similar in their structuring but again differ in the quantitative details. The largest differences between the two distributions are in the regions immediately adjacent to the hydrophobic portions of the solute. Again, this is not surprising given the greater water−water structuring of the SPC/E function, and the fact that water molecules hydrating nonpolar groups structure themselves so as to maximize their hydrogen bonding to other water molecules since they cannot hydrogen bond to the hydrophobic group. As can be seen from Figure 5, there is a much larger cloud of density adjacent to the CH_2 group of carbon C5 than in the TIP3P simulation, and this concentration of density merges with the more extensive cloud of hydrophobic hydration waters below the ring.

Figure 6 displays the anisotropic solvent density calculated from the present SPC/E simulation contoured in a two-dimensional cross section through the approximate plane of the ring (the $x-y$ plane) and in a plane perpendicular to the ring plane. This figure should be compared with Figure 3 of ref 12. This cross-sectional presentation of the data allows the use of multiple contour levels which would be obscured in the three-dimensional figures. Both positive and negative deviations from bulk density are contoured, corresponding to peaks and minima in the solvent distribution. As can be seen, the solvent is extensively structured in a regular fashion dictated by the distribution of functional groups in the solute. In addition to a very ordered ring of first hydration shell peaks in solvent density, there is also a regular array of first minima generally located

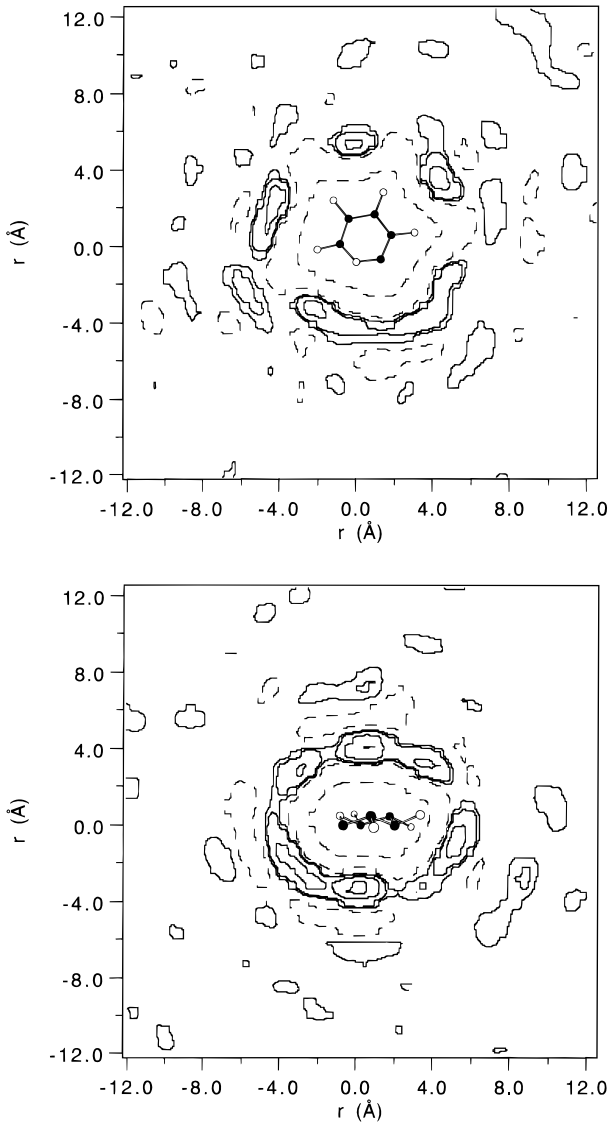

Figure 6. (a, top) Conventional contour map of the density in a two-dimensional cross section through the approximate plane of the ring. Positive deviations from bulk density are contoured with solid lines, while negative deviations are indicated by dashed lines; contours are shown at 90% and 10% below bulk density and 10%, 50%, and 90% above bulk density. (b, bottom) Cross section in a plane perpendicular to the ring.

behind the first maxima peaks, as in the TIP3P simulations, resulting from the partial exclusion of water molecules from these regions due to steric clashes with the water molecules in the first peaks. There is also more extensive structuring, with numerous second hydration peaks beyond the ring of first minima. In general, in the $x-y$ plane (Figure 6a), the first-shell peaks are in the same locations as in the TIP3P simulation, but with a lower intensity, particularly for the peak between the O1 and O2 hydroxyl groups and for the peak between the O4 hydroxyl group and the $C(5)H_2$ group. The first minima are also quite similar between the two simulations, but surprisingly, the array of second-shell density concentrations appears to be less regular in the SPC/E simulation than in the TIP3P study, even though the SPC/E water model is usually thought of as a more structured solvent. It is possible that the stricter local structuring requirements for hydrogen bonding by individual water molecules might inhibit the development of regular long-range structuring around the sugar if the overlapping requirements of that network of peaks were slightly out of register.

The two dimensional cross section in the $y-z$ plane displayed in Figure 6b is again quite similar to the distribution calculated from the TIP3P simulation. Both the peak between the O2 and O3 hydroxyl groups and the hydrophobic hydration peak near the O5−C5 region have shifted somewhat below the plane of the ring, which diminishes their intensity in the cross section presented in Figure 6a. For the density cloud around O5−C5, this shift may have occurred in order to make the interaction with the O5 oxygen atom more tetrahedral; a small peak at the same angle above the plane of the ring is also present in the SPC/E simulation which does not appear in the TIP3P simulation. As with the $x-y$ cross section, there is a general qualitative correspondence with the TIP3P simulation in the distribution of first minima, as would be expected since the positions of these minima are a reflection of the placement of first maxima, which are very similar between the simulations. As in Figure 6a, however, there is again much less direct correspondence between the exact positions of the second-shell maxima between the two calculations.

IV. Conclusions

From the new simulation of β-D-xylopyranose in aqueous solution, it has been confirmed that this sugar imposes considerable structure on its aqueous environment. The principal features of this structuring appear to be determined by geometric considerations dictated by the specific stereochemical architecture of the sugar molecule. Beyond the first hydration shell, however, the extensive solvent structuring observed in both simulations differs as a function of the water model used in the calculations. Presumably the majority of the solution properties of sugar molecules are determined by the direct interactions of the solute molecules with water molecules in the first hydration shells. It is thus encouraging that in these features both simulations are very similar. In particular, recent models of sugar solution properties have suggested that hydration is dominated by such first-shell structuring.[12,28] From our series of simulations of the pyranoid pentoses, we suggested that optimal hydration might be achieved when the solute has a topology which allows the maximum compatibility in the hydration requirements of adjacent functional groups.[12] However, it is possible that the extensive longer-range structuring observed in these simulations also plays an important role in aqueous solvation, and if this is true, then the choice of water potential energy function used to model hydration could be important, since the present calculations reveal differences in this structuring between the SPC/E and TIP3P water models.

Acknowledgment. The authors thank P. A. Karplus and R. K. Schmidt for helpful discussions. This work was supported by grant CHE-9307690 from the National Science Foundation.

References and Notes

(1) Neilson, G. W.; Enderby, J. E. *J. Phys. Chem.* **1996**, *100*, 1317−1322.

(2) Broadbent, R. D.; Neilson, G. W. *J. Chem. Phys.* **1994**, *100*, 7543−7547.

(3) Swaminathan, S.; Harrison, S. W.; Beveridge, D. L. *J. Am. Chem. Soc.* **1978**, *100*, 5705−5712.

(4) Geiger, A.; Rahman, A.; Stillinger, F. H. *J. Chem. Phys.* **1979**, *70*, 263−276.

(5) Nakanishi, K.; Okazaki, S.; Ikari, K.; Touhara, H. *Chem. Phys. Lett.* **1981**, *84*, 428−432.

(6) Cieplak, P.; Kollman, P.; Lybrand, T. *J. Chem. Phys.* **1990**, *92*, 6755−6760.

(7) Kuharski, R. A.; Rossky, P. J. *J. Am. Chem. Soc.* **1984**, *106*, 5786−5793.

(8) Rossky, P. J.; Karplus, M. *J. Am. Chem. Soc.* **1979**, *101*, 1913−1937.

(9) Brady, J. W. *J. Am. Chem. Soc.* **1989**, *111*, 5155−5165.

(10) Brady, J. W.; Schmidt, R. K. *J. Phys. Chem.* **1993**, *97*, 958−966.

(11) Schmidt, R. K.; Karplus, M.; Brady, J. W. *J. Am. Chem. Soc.* **1996**, *118*, 541−546.

(12) Liu, Q.; Brady, J. W. *J. Am. Chem. Soc.* **1996**, *118*, 12276−12286.

(13) Stoddart, J. F. *Stereochemistry of Carbohydrates*; Wiley-Interscience: New York, 1971.

(14) Goldberg, R. N.; Tewari, Y. B. *J. Phys. Chem. Ref. Data* **1989**, *18*, 809−880.

(15) Jorgensen, W. L.; Chandrasekhar, J.; Madura, J. D.; Impey, R. W.; Klein, M. L. *J. Chem. Phys.* **1983**, *79*, 926−935.

(16) Berendsen, H. J. C.; Postma, J. P. M.; van Gunsteren, W. F.; Hermans, J. In *Intermolecular Forces*; Pullman, B., Ed.; Reidel Publishing Co.: Dordrecht, Holland, 1981; pp 331−342.

(17) Berendsen, H. J. C.; Grigera, J. R.; Straatsma, T. P. *J. Phys. Chem.* **1987**, *91*, 6269−6271.

(18) Brooks, B. R.; Bruccoleri, R. E.; Olafson, B. D.; Swaminathan, S.; Karplus, M. *J. Comput. Chem.* **1983**, *4*, 187−217.

(19) Ha, S. N.; Giammona, A.; Field, M.; Brady, J. W. *Carbohydr. Res.* **1988**, *180*, 207−221.

(20) Verlet, L. *Phys. Rev.* **1967**, *159*, 98−103.

(21) van Gunsteren, W. F.; Berendsen, H. J. C. *Mol. Phys.* **1977**, *34*, 1311−1327.

(22) Tasaki, K.; McDonald, S.; Brady, J. W. *J. Comput. Chem.* **1993**, *14*, 278−284.

(23) Joshi, N. V.; Rao, V. S. R. *Biopolymers* **1979**, *18*, 2993−3004.

(24) Brady, J. W. *J. Am. Chem. Soc.* **1986**, *108*, 8153−8160.

(25) Angyal, S. J. *Angew. Chem., Int. Ed. Engl.* **1969**, *8*, 157−226.

(26) Sack, J. S. *J. Mol. Graphics* **1988**, *1988*, 224−225.

(27) Mehrotra, P. K.; Beveridge, D. L. *J. Am. Chem. Soc.* **1980**, *102*, 4287−4294.

(28) Galema, S. A.; Howard, E.; Engberts, J. B. F. N.; Grigera, J. R. *Carbohydr. Res.* **1994**, *265*, 215−225.